

CFD Analysis of the Lateral Sloshing Phenomenon inside an Aerospace LH2 Cryogenic Tank

Matteo CIMINI^{*†}, Francesca Rossetti^{*}, Giacomo Della Posta^{*}, Fulvio Stella^{*} and Matteo Bernardini^{*}

^{*} Sapienza University of Rome

Via Eudossiana 18, 00184 Rome, Italy

matteo.cimini@uniroma1.it – f.rossetti@uniroma1.it – giacomo.dellaposta@uniroma1.it – fulvio.stella@uniroma1.it
– matteo.bernardini@uniroma1.it

[†] Corresponding Author

Abstract

In this work, we propose to perform unsteady 3D numerical simulations by means of the VOF methodology to understand the behavior of the lateral sloshing inside an aerospace LH2 cryogenic tank. The first geometry considered is a simple laboratory-scale cylindrical tank model, designed to investigate the sloshing phenomenon with the presence of a single baffle ring. The case is used to assess the capability of the adopted method to predict the correct sloshing damping. The second geometry under study is instead inspired to a typical common bulkhead cryogenic tank used in space launchers. Simulations investigate sloshing inside the tank under normal gravity conditions. The unsteady lateral force on the tank wall, as well as the center of gravity position, obtained from the simulations are used to obtain and validate a reduced-order model (ROM) that takes into account the non-linear nature of the damping. Lateral loads are then analyzed through Fourier spectral analysis and through wavelet analysis, decomposing the time series into the time-frequency domain, to determine the time evolution of the energy of the excited mode.

1. Introduction

Sloshing occurs when a partially filled reservoir experiences movement or vibration, causing the liquid's unrestrained free surface to move. Lateral sloshing refers specifically to the liquid's motion in response to translational or pitching motions of the reservoir [1]. This type of sloshing creates a standing wave at the liquid-free surface that moves up on one side of the tank and down on the other side in an alternating process over time. The natural frequency of this phenomenon depends on the shape of the tank and the acceleration to which it is subjected, such as gravity acceleration during storage or in a laboratory, or forced acceleration, like the axial acceleration experienced by a space launcher during its ascent phase.

Sloshing is a relevant issue in various fields, including oil and gas and aerospace, with its severity dependent on factors such as the type of application, excitation, and gravitational field. Of these industries, the aerospace sector has particularly emphasized research into sloshing problems, owing to the need to develop high-speed aircraft and large rockets [2-5]. This is because sloshing can significantly impact the dynamics and stability of aerospace vehicles, generating forces and moments that can affect vehicle control and stability, as well as causing damage to tank structures. Sloshing can occur in both liquid and cryogenic tanks, and it can be triggered by factors like changes in vehicle attitude, acceleration, or pressure. The fluid motion can be described using axial, radial, and angular modes, whose relative importance can vary based on tank geometry, fluid properties, and operating conditions. To ensure the safety and efficiency of aerospace tanks, it is crucial to understand sloshing dynamics and develop methods to predict and control it.

Since the early days of the space industry, the dynamics of fluid motion in spacecraft propellant tanks have been the subject of numerous theoretical, experimental, and computational investigations. These analyses have aimed to determine how fluid dynamic loads interact with the vehicle structure and guidance control system. Anti-sloshing devices (ASDs), such as baffles, are the most common means of preventing sloshing inside tanks. Baffles are partitions used to divide the tank into compartments and to keep the liquid in place. Alternatively, adding weight to the bottom of the tank can reduce sloshing by stabilizing it. However, this solution is impractical for space systems due to the crucial weight constraint.

Numerous studies have been conducted over the years to comprehend the physical mechanism of sloshing. Early research on oscillating containers and liquid waves were performed by Hough [6], Honda and Matsushita [7], Taylor [8], Miles and Young [9], among others. However, the Southwest Research Institute (SwRI) played a significant role in advancing this field, with the theoretical work summarized by Abramson [1] being a standard reference for the past six decades. Since then, various numerical, theoretical, and experimental investigations have been undertaken. A number of analytical formulations have been developed by Abramson [10], Bauer [11], Dodge and Garza [12], Stephens and Leonard [13], and numerous experimental campaigns have been conducted in recent decades [14-16]. Several numerical studies have exploited CFD simulations to forecast the sloshing phenomenon [17-20]. The complexity of fluid dynamics poses one of the primary challenges in predicting and controlling sloshing. Reduced order models (ROMs) have been proposed as practical tools for simulating and predicting the sloshing dynamics. ROMs are mathematical models that represent the system's behavior with a small number of parameters, resulting in a reduced computational cost. These approaches can offer a simplified but accurate representation of fluid dynamics and can be used to predict the system's response to different disturbances. Examples of ROMs employed to describe sloshing include the spring-mass model [21, 22], the pendulum model [19], the Galerkin method [23, 24], proper orthogonal decomposition (POD) [24, 25], and balanced truncation [26]. Neural network ROM models have also been proposed and tested in the research community recently [27-30]. This brief overview covers only a fraction of the vast body of work conducted on sloshing. Ibrahim, Pilipchuk, and Ikeda [31] provide a comprehensive discussion of recent advances in sloshing.

This paper presents a study focusing on a common bulkhead cryogenic LH2 tank, equipped with two ASD ring, a typical configuration used in the aerospace sector. In particular, three-dimensional, two-phase, unsteady, laminar CFD numerical simulations exploiting the Volume-of-Fluid (VOF) methodology are carried out to predict lateral forces. The primary aim of the study is to find a calibrated pendulum ROM model by analyzing the time history of the lateral force and the propellant CoG movement. The manuscript is organized as follows: Sec. 2 outlines the methodological approach and computational setup, as well as a validation test case on a cylindrical tank with a flat bottom and a single ASD ring. Sec. 3 presents the main findings of the study, including results at two different filling levels. Finally, the conclusions are discussed in Sec. 4.

2. Computational Setup and Validation

2.1 Flow Solver and Numerical Approach

The VOF model has been used in the three-dimensional unsteady simulations to track the two-phase fluid interface. Both phases are assumed to be incompressible, laminar, and immiscible with a sharp interface, with a surface tension between the two phases set to 0.0011784 N/m (LH2, see Sec. 2.2). The Navier-Stokes (NS) equations have been solved using the commercial CFD solver ANSYS Fluent® [32]. A pressure-based solver has been used for all the simulations with the SIMPLE algorithm. The momentum equations have been discretized using a second-order scheme, while the VOF equation has been discretized using a Compressive scheme. The time formulation used is second-order implicit, and a time step of $\Delta t = 0.001$ s has been selected after performing a time-step convergence study. The tank walls are considered adiabatic with no slip for all cases analyzed.

2.2 Tank configuration and Operating Conditions

The tank in this study is a typical aerospace common bulkhead reservoir filled with a liquid cryogenic propellant under normal gravity ($g_0 = 9.81$ m/s²). It has a radius $R = 1.2$ m, and it is equipped with two ASD rings positioned at $h/R = 0.8$ and 1.2 , respectively. Both the devices are 0.25 m wide ($w/R = 0.2$) and 0.022 m thick. A schematic representation of the tank is shown in Fig. 1. To avoid the computational effort related to the vapor phase in the ullage, the upper part of the tank is neglected from the sloshing computation and therefore the geometry has been cutted at $h/R = 1.5$. The tank is filled with liquid hydrogen (LH2) at the pressure of 3 bar and a temperature of 24.68 K. Under this condition, the propellant has a density $\rho_{LH2} = 65.19$ kg/m³ and a viscosity $\mu_{LH2} = 9.6807e-06$ Pa·s. The vapor phase comprises gaseous hydrogen, which has a density $\rho_{GH2} = 3.64$ kg/m³ and a viscosity $\mu_{GH2} = 1.2536e-06$ Pa·s. The sloshing phenomenon has been studied through a free-decay technique, by imposing an initial inclination of 5°, with respect to the horizontal free surface.

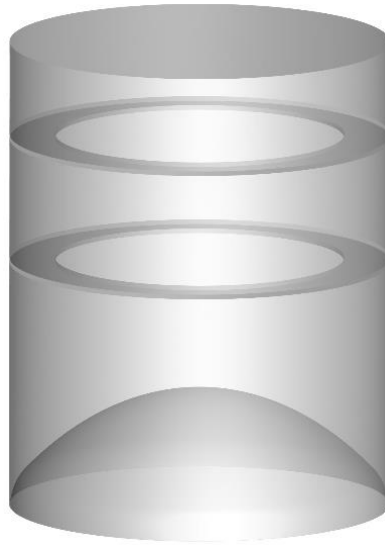


Figure 1: Schematic of the common bulkhead LH2 tank used in this study. Ullage zone cutted to minimize computational time.

2.3 Meshing Strategy

The entire computational domain is discretized with a hybrid structured-unstructured approach. The structured part is composed of a series of wall-orthogonal inflation layers starting from all the walls, with the first cell height of $\Delta s_0 = 1e - 04$ m. The unstructured part is composed of polyhedral cells that begins when the structured layer reaches the cell isotropy on average. An overview of the computational grid is provided in Fig. 2. A local mesh refinement near the free surface and near the first baffle ring from the bottom has been implemented, which is necessary to capture the interface and accurately predict the vortex shedding phenomenon. The final mesh is composed of 2M cells in total.

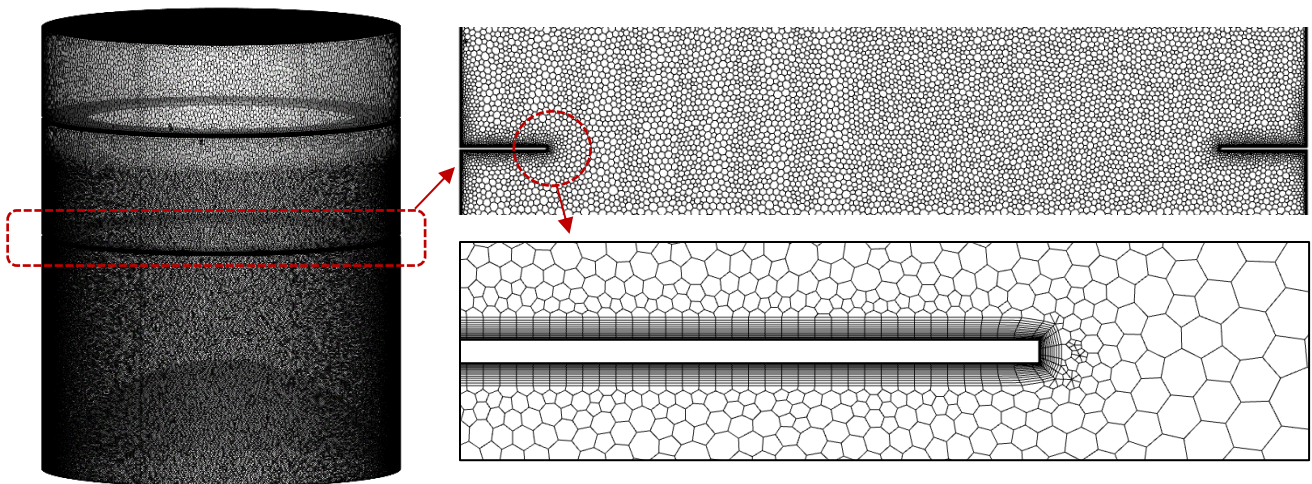


Figure 2: Three-dimensional visualization of the polyhedral mesh of the common bulkhead LH2 tank.

2.4 Validation Test Case: Cylindrical Tank with ASD Ring

ASD baffles are usually placed at the tank walls to provide the damping necessary to meet stability requirements and prevent instabilities in the control system. As known in the literature, a flat ring baffle is the most efficient and most frequently used ASD system in cylindrical tanks [1]. The ASD ring damping can be determined by using the Miles equation [33], which can be expressed as

$$\gamma_{Miles} = \frac{15 \left(\frac{4}{3\pi}\right)^2 \alpha A e^{-4.601 d/R} \sqrt{\eta w}}{2\sqrt{\pi} \left(\frac{m_s}{\rho}\right) \Gamma^2}, \quad (1)$$

where γ_{Miles} is the Miles equation ASD ring ramping, A is the tank cross section, d is the depth of the baffle below the free surface, w is the ring width, Γ is the ratio between the lateral displacement of the sloshing mass and the sloshing wave amplitude η , and α is the ratio between the ring area and the tank cross section, A , defined in a cylindrical tank. The latter can be expressed as

$$\alpha = \frac{2w}{R} - \frac{w^2}{R^2}. \quad (2)$$

It is clear from the Miles equation that the dependency of the baffle damping on the sloshing wave amplitude is a crucial point of ASD damping.

To investigate the sloshing phenomenon in a cylindrical tank and understand the impact of the ASD on damping and vortex shedding, we propose the validation test case depicted in Fig. 3. This case involves various filling levels ($h/R = 2.16$, $h/R = 2.23$, and $h/R = 2.36$) to explore the influence of the ASD ring on damping. The experimental campaign of Perez et al. [14] has been replicated to verify the methodology accuracy in capturing the high level of damping anticipated in these scenarios and the ASD tip's vortex shedding. The tank has a radius $R = 0.5461$ m, and the ASD ring is positioned at $h_{ASD}/R = 2.04$. The wing is 0.112 m wide ($w/R = 0.204$) and 0.003 m thick. The cylindrical tank is filled with water ($\rho_{H2O} = 998.2$ kg/m³, $\mu_{H2O} = 1e-3$ Pa·s) at ambient temperature, and the experiment is conducted under normal gravity ($g_0 = 9.81$ m/s²). The vapor phase comprises air at ambient temperature ($\rho_{air} = 1.225$ kg/m³, $\mu_{air} = 1.79e-5$ Pa·s). The sloshing phenomenon is investigated using a free-decay approach, and Table 1 provides information about the initial angle and the corresponding ratio between the free surface height and the tank radius (η/R).

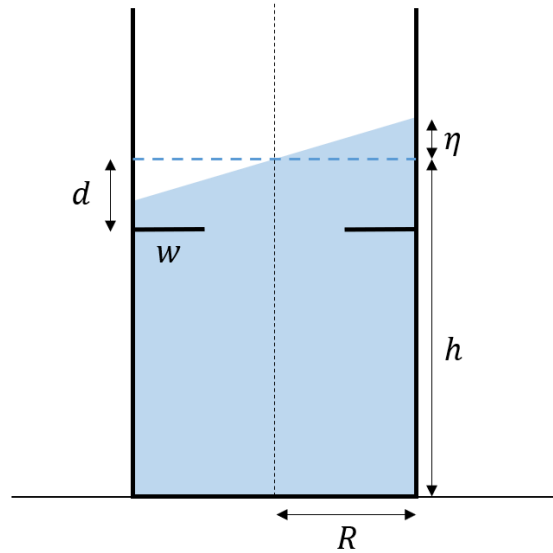


Figure 3: Schematic of lateral sloshing in a cylindrical tank with the presence of an ASD ring.

Table 1: Cylindrical tank with an ASD ring: initial slope at different h/R .

h/R	η/R	Initial slope
2.16	0.0669	3.83°
2.23	0.0766	4.38°
2.36	0.0456	2.61°

The results of the validation test case with a single ASD ring are presented in Fig. 4, which displays the time history of the lateral force in the x-direction for the different h/R ratios investigated. A straight line connecting the first two peaks in the lateral force plot has been added to emphasize the damping level in the different cases, which is proportional to the slope of the line. The figure demonstrates that as h/R increases, damping decreases due to the reduced effect of the ASD on the fluid. When h/R is 2.16, the free surface is close to the ASD, and a significant vortex shedding phenomenon emerges from the ring tip, which increases damping by interacting with the free surface. Conversely, when h/R is 2.36, the vortices detached from the ring tip are smaller, resulting in lower damping. Therefore, the damping value is directly related to the intensity of eddies vorticity. The damping factor evaluated on the first two peaks is $\gamma = 8.21\%$ for $h/R = 2.16$, $\gamma = 5.55\%$ for $h/R = 2.23$, and $\gamma = 1.74\%$ for $h/R = 2.36$. The obtained damping values are compared with those in the literature in Table 2 and Fig. 5, showing an excellent agreement with the experimental data of Perez et al. [14] for all h/R , with slight deviations. The largest deviation from the experimental data is found in the case with $h/R = 2.36$, (14.9% error). Nonetheless, this value is within the uncertainty range typically assumed in the literature, and as shown in Fig. 5, the present outcomes are capable of representing the Miles equation with less than 1% difference. It is important to note that, in this particular case with the ASD, the smooth-wall viscous damping is still present, but its impact is negligible compared to the high-level damping generated by the ring. This is demonstrated by the fourth point at $h/R = 2$ in Fig. 5, where the free surface level is below the ring and the ASD is not operating. In this scenario, the entire damping is created by the smooth walls.

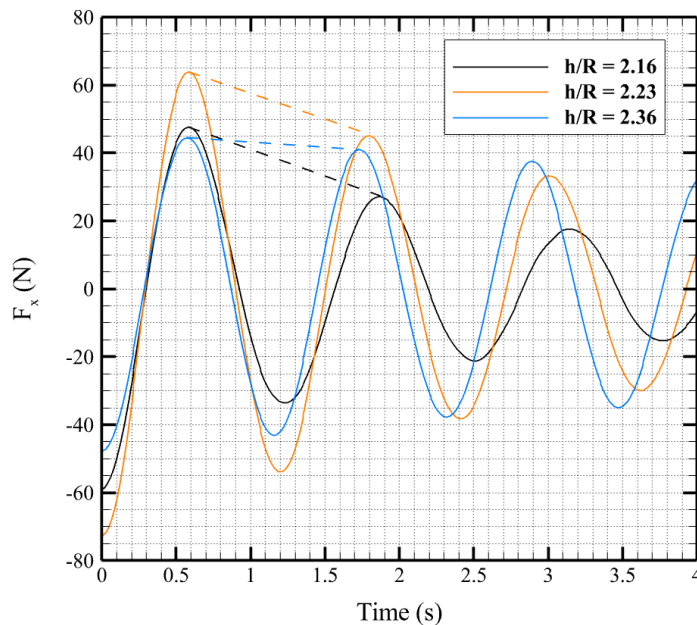


Figure 4: Validation test case: time history of the lateral force.

Table 2: Validation test case: Comparison of the damping ROM parameter with the literature results.

h/R	Present CFD	Pérez (Exp.)	Miles (An.)
2.16	8.21	7.95 (3.2%)	8.51 (3.7%)
2.23	5.55	5.23 (5.8%)	5.69 (2.5%)
2.36	1.74	2.00 (14.98%)	1.75 (0.6%)

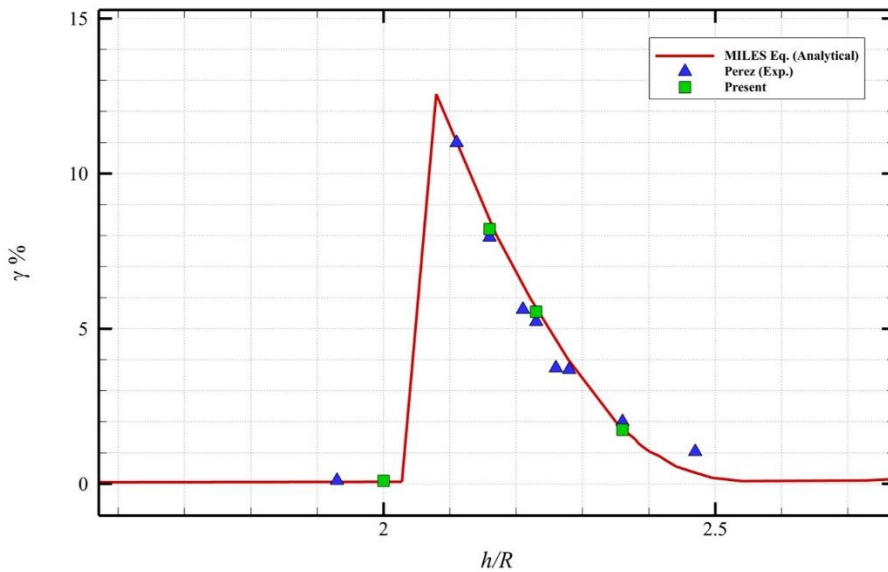


Figure 5: Validation test case: comparison of the damping factor parameter with the literature data.

3. Results

3.1 High Filling Level

The results of the LH2 common bulkhead tank are reported in Fig. 6, which shows the time history of the lateral force at $h/R=1.25$ (almost full filling). In the same figure, the comparison of the CFD data with the force obtained with the pendulum ROM model is shown, where it is possible to notice that an excellent agreement has been achieved. Nevertheless, some discrepancies arise for $t > 5$ s, due to the non-linearity of the damping in the presence of ASD rings. However, it is worth noticing that in the presence of this ring baffle, the main frequency of the sloshing wave is not altered (softening effect). To ensure this, an FFT, a PSD and a Continuous Wavelet analysis of the force signal have been performed, whose results are shown in Fig. 7, Fig. 8 and Fig. 9.

Wavelet analysis is becoming a common tool to analyze localized variations of power within signals. By decomposing time series into the time-frequency domain, one is able to determine both the dominant modes of variability and how those modes vary in time. The results of the wavelet analysis are usually reported in terms of the Wavelet Power Spectrum (WPS) normalized by the variance σ^2 of the transformed signal, describing how the variance is distributed in frequency. As can be seen, the FFT analysis shows a single and clear peak at $f \approx 0.5$ Hz, which is the frequency extracted from the CFD raw data for the ROM model. Also in this case, the comparison between the pendulum model and the numerical simulation shows an excellent agreement. The same results is obtained for the PSD of Fig. 8. The Wavelet analysis shows that the frequency does not change in time, as expected, and that the sloshing wave amplitude is damped in time. However, the WPS results are out the cone of influence of the wavelet analysis, meaning that a longer simulation is needed to obtain a more robust result.

The damping factor evaluated on the first two peaks [14] is $\gamma = 9.37\%$. The remaining extrapolated ROM parameters are provided in Table 3.

Table 3: LH2 Tank with high h/R: extracted ROM parameters.

f (Hz)	γ %	m_p/m_{tot}	m_0/m_{tot}	H_p/R	H_0/R	L_p/R
0.5	9.37	0.38	0.62	0.34	1.94	0.83

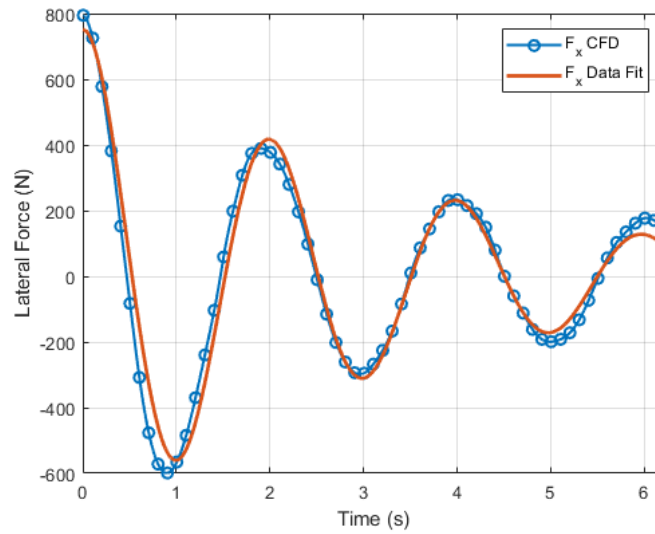


Figure 6: LH2 Tank with high h/R: time history of the lateral force. The figure shows the comparison between the CFD data and the ROM data fit.

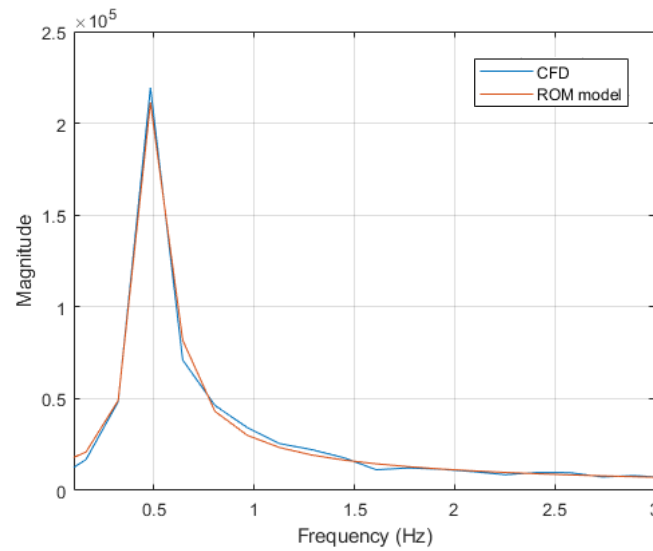


Figure 7: LH2 Tank with high h/R: FFT of the lateral force signal. The figure shows the comparison between the CFD data and the ROM data fit.

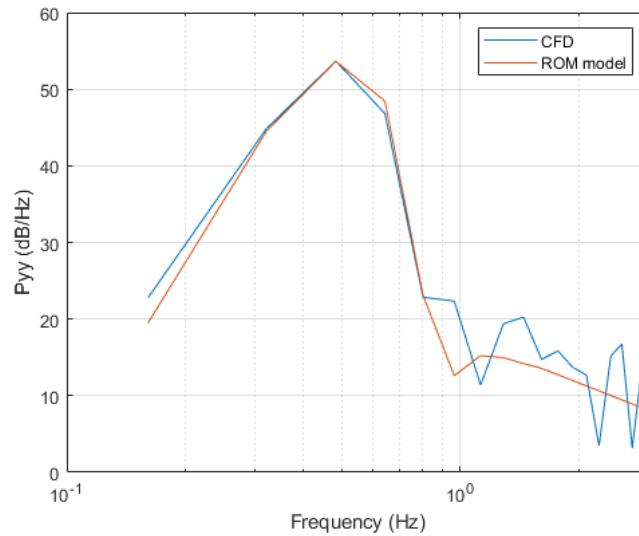


Figure 8: LH2 Tank with high h/R: PSD of the lateral force signal. The figure shows the comparison between the CFD data and the ROM data fit.

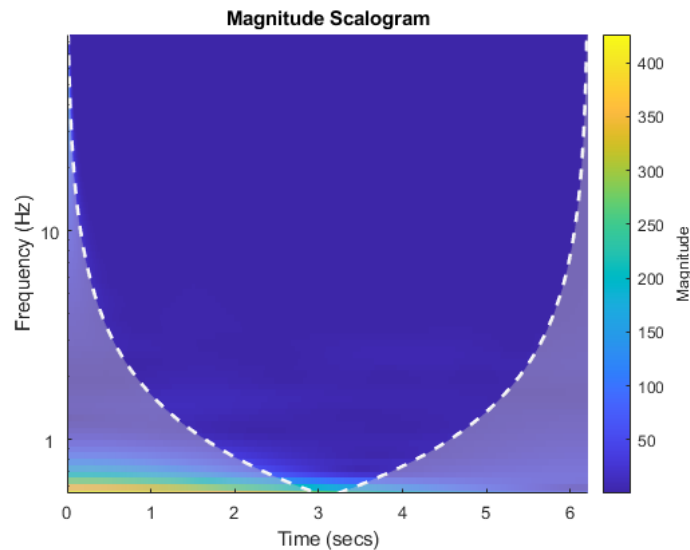


Figure 9: LH2 Tank with high h/R: Wavelet (WPS) of the lateral force signal.

3.2 Low Filling Level

The results of the second case of the lateral sloshing inside a LH2 common bulkhead tank are reported in Fig. 10, which shows the time history of the CoG x coordinate, at $h/R=0.52$ (low filling level). In the same figure, the comparison of the CFD data with the CoG position obtained with the pendulum ROM model shows a good agreement with some discrepancies arising at almost all peaks.

Differently from the previous case, the slosh wave is not strongly damped, due to the fact that at this filling level the LH2 propellant free surface is below the two ASD rings and the only damping effect is produced by the viscous walls. Also in this case, the main frequency of the sloshing wave is not subjected to softening effects, as shown by the WPS of Fig. 11. In fact, the figure shows a strong and persistent peak at $f \approx 0.37$ Hz that does not decrease its magnitude in time, due to the presence of only the wall viscous damping. However, the same figure shows some weak traces of physical phenomena at higher frequencies. The FFT analysis of Fig. 12 shows the presence of two peaks, the first at $f \approx 0.37$ Hz, and the second between $1 < f < 1.2$ Hz. In this case, the comparison between the pendulum model and the numerical simulation shows an excellent agreement for the first peak but the ROM model is not able to capture the second peak, since it is composed of only one pendulum mass. The same outcome is obtained for the PSD of Fig. 13.

It is worth noticing that the same case simulated with a flat bottom does not produce the appearance of this second peak at higher frequency. Moreover, with a flat bottom, the damping obtained from the CoG signal is 7% less. We can conclude that the presence of the second peak, as well as the greater damping, is a consequence of the presence of the common bulkhead bottom, which induces non-linear effects on the sloshing wave with its curvature. Moreover, since at the center of the tank, the bottom is closer to the free surface, the damping effect increases [14]. The damping factor evaluated is $\gamma = 0.001\%$. The remaining extrapolated ROM parameters are provided in Table 4.

Table 4: LH2 Tank with low h/R: extracted ROM parameters.

f (Hz)	γ %	m_p/m_{tot}	m_0/m_{tot}	H_p/R	H_0/R	L_p/R
0.37	0.001	0.51	0.49	0.16	3.3	1.54

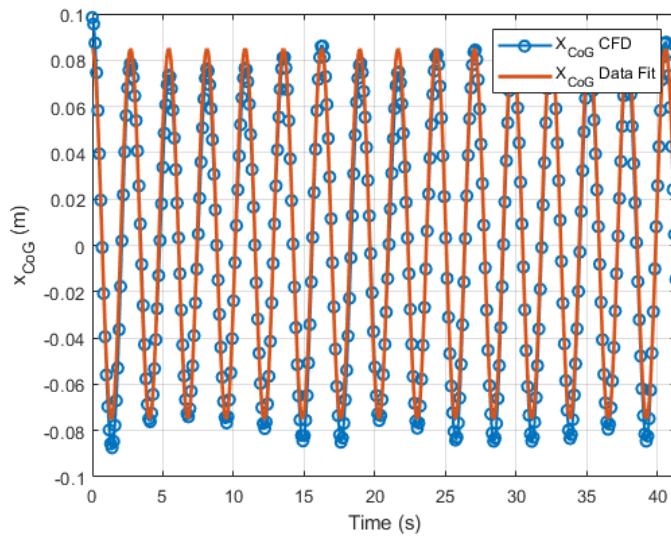


Figure 10: LH2 Tank with low h/R: time history of the lateral force. The figure shows the comparison between the CFD data and the ROM data fit.

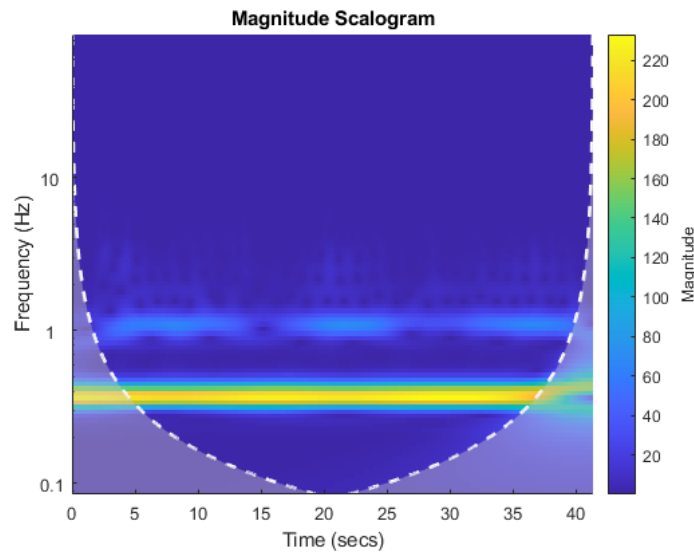


Figure 11: LH2 Tank with low h/R: Wavelet (WPS) of the lateral force signal.

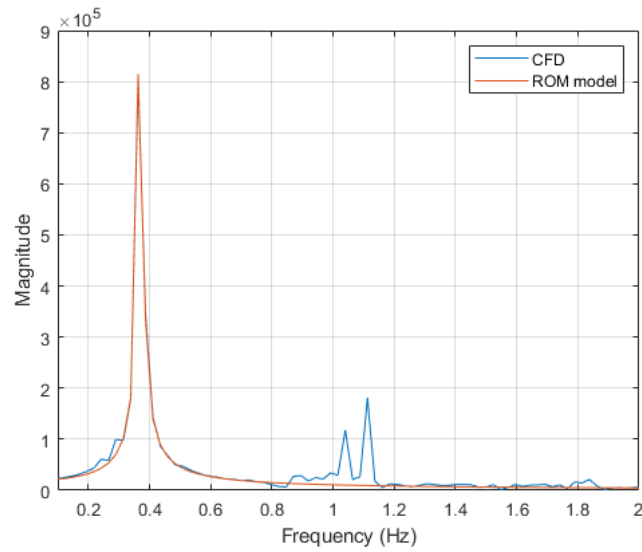


Figure 12: LH2 Tank with low h/R : FFT of the lateral force signal. The figure shows the comparison between the CFD data and the ROM data fit.

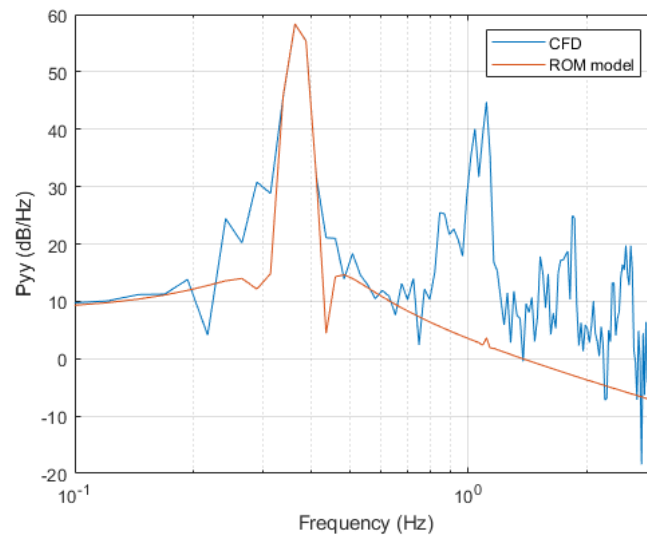


Figure 13: LH2 Tank with low h/R : PSD of the lateral force signal. The figure shows the comparison between the CFD data and the ROM data fit.

4. Conclusions

In this study, we investigated the sloshing phenomenon within a three-dimensional, two-phase, unsteady, cryogenic LH2 tank with a common bulkhead bottom and under normal gravity conditions by means of CFD simulations. The tank is equipped with two ASD ring, as typically found in tanks used in the aerospace field for space launchers. Initially, we studied a cylindrical tank with flat bottom, reproducing the experimental campaign of [14], in order to validate the numerical methodology and computational grid used. Our findings exhibited excellent agreement with both experimental data and predictions from the Miles equation.

Once the model was validated, we performed free-decay sloshing CFD simulations on the real tank filled with cryogenic LH2 propellant at two different filling levels. The first filling level under investigation was with the tank almost full and the LH2 free surface just above the upper ASD ring. In this configuration, the vortex shedding produced at the ring tip is able to strongly damp the sloshing phenomenon. The pendulum ROM parameters obtained are in

excellent agreement with the CFD data and the frequency analysis shows the presence of a single constant frequency peak with a decreasing magnitude in time, as expected.

In the second filling level investigated, on the contrary the tank was almost empty, with the LH2 free surface under both the ASD ring and just above the common bulkhead bottom surface. In this case, only the wall viscous damping is able to act on the sloshing wave. The frequency analysis highlights the presence of two peaks, one related to the main frequency of the lateral sloshing wave and one, at higher frequency, due to the presence of the curved bottom surface. The curvature of the lower part of the tank, seems to induce non-linear effects on the sloshing wave and also tends to increase the damping level by a 7% factor with respect to the same case with a flat bottom.

References

- [1] H. N. Abramson, “The dynamic behavior of liquids in moving containers, with applications to space vehicle technology,” Tech. Rep. (1966).
- [2] A. A. Schy, A theoretical analysis of the effects of fuel motion on airplane dynamics, Vol. 1080 (National Advisory Committee for Aeronautics, 1951).
- [3] J. L. Sewall, “An experimental and theoretical study of the effect of fuel on pitching translation flutter,” Tech. Rep. (1957).
- [4] H. N. Abramson and L. R. Garza, “Liquid frequencies and damping in compartmented cylindrical tanks,” *Journal of Spacecraft and Rockets* 2, 453–455 (1965).
- [5] H. F. Bauer, “Theory of fluid oscillations in partially filled cylindrical containers,” MSFC, Rept. No. MTP-AERO-62-1, (Jan. 1962) 4 (1962).
- [6] S. S. Hough, “Xii. the oscillations of a rotating ellipsoidal shell containing fluid,” *Philosophical Transactions of the Royal Society of London. (A.)*, 469–506 (1895).
- [7] K. Honda and T. Matsushita, “An investigation of the oscillations of tank water,” *Sci. Rep. Tohoku, Imp. Univ., First Ser* 21, 131–148 (1913).
- [8] G. I. Taylor, “The instability of liquid surfaces when accelerated in a direction perpendicular to their planes. i,” *Proceedings of the Royal Society of London. Series A. Mathematical and Physical Sciences* 201, 192–196 (1950).
- [9] J. Miles and D. Young, “Generalized Missile Dynamics Analysis. IV. Sloshing,” Tech. Rep. (TRW Space Technology Labs Los Angeles Calif, 1958).
- [10] H. N. Abramson, “Liquid dynamic behavior in rocket propellant tanks,” in *ONR/AIA Symposium on Structural Dynamics of High Speed Flight* (1961) pp. 287–318.
- [11] H. F. Bauer, “Dynamics of liquid propellant vehicles,” in *Office of Naval Research/Aerospace Industries Association Symposium on Structural Dynamics of High Speed Flight*, Los Angeles, Calif (1961) pp. 319–355.
- [12] F. T. Dodge and L. R. Garza, “propellant dynamics in an aircraft-type launch vehicle,” Tech. Rep. (1971).
- [13] D. G. Stephens and H. W. Leonard, *The Coupled Dynamic Response of a Tank Partially Filled with a Liquid and Undergoing Free and Forced Planar Oscillations* (National Aeronautics and Space Administration, 1963).
- [14] J. G. Perez, R. Parks, D. R. Lazor, et al., “Validation of slosh model parameters and antislosh baffle designs of propellant tanks by using lateral slosh testing,” in *28th Aerospace Testing Seminar*, M12-1999 (2012).
- [15] D. G. Stephens, H. W. Leonard, and T. W. Perry Jr, “Investigation of the damping of liquids in right-circular cylindrical tanks, including the effects of a time-variant liquid depth,” Tech. Rep. (1962).
- [16] F. Saltari, M. Pizzoli, G. Coppotelli, F. Gambioli, J. E. Cooper, and F. Mastroddi, “Experimental characterisation of sloshing tank dissipative behaviour in vertical harmonic excitation,” *Journal of fluids and structures* 109, 103478 (2022).
- [17] H. Yang and J. Peugeot, “Propellant sloshing parameter extraction from computational fluid-dynamics analysis,” *Journal of Spacecraft and Rockets* 51, 908–916 (2014).
- [18] H. Yang, R. Purandare, J. Peugeot, and J. West, “Prediction of liquid slosh damping using a high resolution CFD tool,” in *48th AIAA/ASME/SAE/ASEE Joint Propulsion Conference & Exhibit* (2012) p. 4294.

- [19] S. T. Green, “A comparison of methods for estimating slosh model parameters from CFD simulations,” in 2018 Joint Propulsion Conference (2018) p. 4758.
- [20] B. Marsell, S. Gangadharan, Y. Chatman, J. Sudermann, K. Schlee, and J. Ristow, “A CFD approach to modeling spacecraft fuel slosh,” in 47th AIAA Aerospace Sciences Meeting including the New Horizons Forum and Aerospace Exposition (2009) p. 366.
- [21] M. Pizzoli, F. Saltari, and F. Mastroddi, “Linear and nonlinear reduced order models for sloshing for aeroelastic stability and response predictions,” *Applied Sciences* 12, 8762 (2022).
- [22] M. Colella, F. Saltari, M. Pizzoli, and F. Mastroddi, “Sloshing reduced-order models for aeroelastic analyses of innovative aircraft configurations,” *Aerospace Science and Technology* 118, 107075 (2021).
- [23] F. Pochet, K. Hillewaert, P. Geuzaine, J.-F. Remacle, and E. Marchandise, “A 3D strongly coupled implicit discontinuous galerkin level set-based method for modeling two-phase flows,” *Computers & Fluids* 87, 144–155 (2013).
- [24] D. Amsallem and C. Farhat, “On the stability of reduced-order linearized computational fluid dynamics models based on pod and galerkin projection: descriptor vs non-descriptor forms,” *Reduced order methods for modeling and computational reduction*, 215–233 (2014).
- [25] K. Willcox and J. Peraire, “Balanced model reduction via the proper orthogonal decomposition,” *AIAA journal* 40, 2323–2330 (2002).
- [26] D. Amsallem and C. Farhat, “Projection-based model reduction with stability guarantee,” in 6th AIAA Theoretical Fluid Mechanics Conference (2011) p. 3113.
- [27] F. Saltari, A. Traini, F. Gambioli, and F. Mastroddi, “A linearized reduced-order model approach for sloshing to be used for aerospace design,” *Aerospace Science and Technology* 108, 106369 (2021).
- [28] M. Pizzoli, F. Saltari, F. Mastroddi, J. Martinez-Carrascal, and L. M. González-Gutiérrez, “Nonlinear reduced-order model for vertical sloshing by employing neural networks,” *Nonlinear dynamics*, 1–10 (2022).
- [29] M. Pizzoli, F. Saltari, G. Coppotelli, and F. Mastroddi, “Neural network-based reduced-order modeling for nonlinear vertical sloshing with experimental validation,” *Nonlinear Dynamics*, 1–21 (2023).
- [30] F. Saltari, M. Pizzoli, F. Gambioli, C. Jetzschmann, and F. Mastroddi, “Sloshing reduced-order model based on neural networks for aeroelastic analyses,” *Aerospace Science and Technology* 127, 107708 (2022).
- [31] R. A. Ibrahim, V. N. Pilipchuk, and T. Ikeda, “Recent advances in liquid sloshing dynamics,” (2001).
- [32] I. Ansys, “Ansys fluent theory guide,” Canonsburg, Pa 794 (2011).
- [33] J. W. Miles, “On the sloshing of liquid in a cylindrical tank,” Tech. Rep. (Thompson Ramo Wooldridge Inc Los Angeles CA, 1956).